JOURNAL OF MATERIALS SCIENCE 31 (1996) 3929–3936

Precipitation characteristics of μ-phase in wrought nickel-base alloys and its effect on their properties

H. M. TAWANCY
Materials Characterization Laboratory Metrology, Standards, and Materials Division, Research Institute, King Fahd University of Petroleum and Minerals, P.O. Box 1639, Dhahran 31261, Saudi Arabia

Thermal exposures consisting of 1–16 000 h at 540, 650, 760, and 870 °C were used to study the susceptibility of selected nickel-base alloys to precipitation of μ-phase and its effect on mechanical strength and corrosion resistance. Analytical electron microscopy and X-ray diffraction were used to characterize the μ-phase. A μ-phase of the type Mo_6Ni_7 in nickel-base alloys was found to be stabilized by critical concentrations of iron in an excess of about 3 wt%. Generally, the μ-phase had a characteristic defect structure consisting of twins and stacking faults, and it exhibited a preferential tendency for precipitation at existing molybdenum-rich carbide particles within the alloy matrix and at grain boundaries. Precipitation of μ-phase was found to produce a moderate loss of room-temperature tensile ductility; however, it resulted in a considerable degradation of impact toughness and corrosion resistance. In contrast, it had no significant effect on elevated temperature tensile properties. A correlation was found to exist between the Ni/Fe + Co ratio as well as the Mo + W content of the alloy and susceptibility to precipitation of μ-phase.

1. Introduction

Long-term microstructural stability is one of the important parameters determining the suitability of engineering alloys for continuous use at elevated temperatures, (e.g. [1]). This can be limited by precipitation of secondary phases degrading their mechanical strength and/or environmental resistance, particularly a group of intermetallic compounds commonly known as topologically close-packed phases (TCP) because of their characteristic crystal structures, e.g. σ, Laves, and μ-phases [1–3]. In practice, the approach of electron hole number, ($\bar{N}_v$, is used to control the precipitation of TCP phases, particularly the σ-phase by adjusting the alloy composition [2]. However, in general, it is not possible to predict the occurrence of μ- and Laves phases on the basis of the $\bar{N}_v$ approach [2].

It is well known that the μ-phase (A_6B_7-type composition where A is molybdenum and/or tungsten and B is iron and/or cobalt) has a hexagonal close-packed structure $D8_5$ crystal system; 39 atoms/unit cell) with lattice constants of $a = 0.476$–0.479 nm and $c = 2.57$–2.59 nm depending upon the exact chemical composition [3, 4]. Previous work had shown that the μ-phase is preferentially formed at electron concentrations (e/a) in the range of 7.1–8.0 [3–5]. Because of the relatively high electron-to-atom ratio of nickel (e/a = 10), it deters the formation of μ-phase and therefore, a μ-phase of the type Mo_6Ni_7 or W_6Ni_7 where e/a = 8.15 is not expected to be stable [3]. Also, the susceptibility to precipitating μ-phase is decreased as tantalum, niobium and titanium are substituted for molybdenum and tungsten [3, 4].

It is was the objective of this study to examine the susceptibility of selected nickel-base alloys of commercial grades to precipitation of μ-phase upon exposure to elevated temperatures. Emphasis was placed upon the microstructural features of μ-phase and its effect on mechanical strength and corrosion resistance as well as the compositional parameters influencing its precipitation.

2. Experimental procedure

Ten nickel-base alloys of commercial grades (Hastelloy® alloys B, B-2, C, C-276, C-4, C-22, and X, and Haynes® alloys 230 and 625) were included in this study representing the heat-resistant alloys S, X, 230, and 625, and corrosion-resistant alloys B, B2, C, C-276, C-4 and C-22 (R = registered trademarks of the Haynes International Company, Kokomo, Indiana). Table I summarizes the chemical compositions of the heats of alloys studied in comparison with their nominal chemical compositions. As can be seen, alloys B and B2 are based upon the Ni–Mo system while alloys C, C-276, C-4, C-22, S, and 625 are based upon the Ni–Mo–Cr system. Two heats of alloy 625 were included in the study to demonstrate the effect of the exact iron content. Alloy 230 is based upon the Ni–W–Cr system and alloy X is based upon the Ni–Mo–Cr–Fe system.

0022–2461

TABLE I Chemical compositions (wt%) of the heats of alloys studied. Nominal compositions in parentheses

Alloy	Ni	Mo	Cr	W	Nb + Ta	Fe	Co	C
B	Bal.	27.76 (28)	0.7 (1[a])	–	–	5.66 (5)	0.61 (2.5[a])	0.02 (0.05[a])
B2	Bal.	26.57 (28)	0.1 (1[a])	–	–	0.91 (2[a])	0.1 (1[a])	0.002 (0.01[a])
C	Bal.	16.05 (16)	15.6 (15.5)	3.7 (3.75)	–	5.15 (5.5)	1.3 (2.5[a])	0.03 (0.08[a])
C-276	Bal.	16.19 (16)	15.01 (15.5)	3.33 (3.75)	–	5.39 (5.5)	1.01 (2.5[a])	0.002 (0.01[a])
C-4	Bal.	15.99 (16.5)	16.06 (16)	–	–	0.72 (3[a])	0.12 (2.5[a])	0.002 (0.01[a])
C-22	Bal.	12.96 (13)	21.97 (22)	2.91 (3)	–	3.1 (3)	1.07 (2.5[a])	0.002 (0.01[a])
S	Bal.	15.19 (15.25)	15.14 (15.25)	0.25 (1[a])	–	1.1 (3[a])	0.23 (2[a])	0.007 (0.02[a])
X	Bal.	8.75 (9)	21.09 (21.75)	0.39 (0.8)	–	18.82 (18.5)	1.71 (1.5)	0.09 (0.1)
230	Bal.	1.89 (2)	21.76 (22)	13.78 (14)	–	2.05 (3[a])	2.43 (5[a])	0.07 (0.1)
625	Bal.	9.05 (9)	20.67 (21.5)	–	3.63 (3.65)	3.49 (5[a])	0.21 (1[a])	0.06 (0.1)
	Bal.	8.89	20.94	–	3.60	2.31	0.24	0.05

[a]Maximum.

All alloys were in the form of 2–3 mm thick mill-annealed sheets and 12.7 mm thick plates. To determine their susceptibility to precipitation of μ-phase, samples were exposed for 1 h and up to 16 000 h at 540, 650, 760 and 870 °C followed by water quenching. Both X-ray diffraction (XRD) and analytical electron microscopy (AEM) were used to identify the μ-phase. Transmission and scanning transmission electron microscopy (TEM/STEM) modes of AEM were used to characterize the microstructure of μ-phase at 200 keV. Thin foils were prepared by the jet polishing technique in a solution consisting of 30% nitric acid in methanol and maintained at about − 20 °C. Room- and elevated-temperature tensile tests as well as Charpy impact tests were used to determine the effect of μ-phase precipitation on mechanical strength. Tensile tests were carried out on sheet samples (50.8 mm gauge length) and plate samples were used in the impact tests. Aqueous corrosion tests were carried out on coupons 25.4 mm × 25.4 mm × 2–3 mm by 24 h immersion in boiling 10% HCl (reducing medium) as well as in boiling H_2SO_4 + 42 g/l^{-1} ferric sulphate (oxidizing medium) to determine the effect of μ-phase precipitation on corrosion resistance.

Because the microstructural features of μ-phase and the corresponding effects on properties were found to be rather similar in the susceptible alloys, representative examples are presented below. However, specific differences from one alloy to another are pointed out.

3. Results and discussion

3.1. Susceptibility to precipitation of μ-phase

Examination of specimens exposed for up to 16 000 h at 540, 650, 870 and 980 °C by XRD and AEM revealed that μ-phase had formed in alloys C, C-276, C-22, B, and X. In the case of alloy 625, the susceptibility to precipitation of μ-phase was found to be dependent upon the exact iron content. In contrast, at all temperatures studied, there was no evidence for the presence of μ-phase in alloys C-4, S, 230, and B2 after up to 16 000 h exposure as summarized in Table II.

Alloys C, C-276, C-22, and 625 based upon the Ni–Mo–Cr system exhibited a similar behaviour in that the μ-phase was found to precipitate at all the temperatures studied. However, the precipitation kinetics were accelerated at 870 °C where substantial amounts of μ-phase were observed after 1 h of exposure. In contrast, precipitation of μ-phase in alloy X (Ni–Mo–Cr–Fe) was more pronounced at 870 °C. However, the kinetics were rather sluggish in comparison with the Ni–Mo–Cr alloys. In this case, marked precipitation occurred after 1000 h exposure at 870 °C. A different behaviour was exhibited by alloy B where precipitation of μ-phase was detected only at 540 and 650 °C after at least 1000 h exposure.

TABLE II Susceptibility of the alloys studied to precipitation of μ-phase based upon 16 000 h exposure at 540–670 °C

Alloy	μ-phase
B	Yes
B2	No
C	Yes
C-276	Yes
C-4	No
C-22	Yes
S	No
X	Yes
230	No
625	No (≤ 3% Fe) Yes (> 3% Fe)

Because relevant phase-diagram data for the above alloys are rather scarce, it was not possible to correlate the above observations with phase stability characteristics. However, as shown later, the above differences in behaviour could be correlated at least partially with variations in concentrations of μ-forming elements, particularly molybdenum, tungsten and iron.

3.2. Microstructural features of μ-phase

Analysis of XRD data revealed that the μ-phase formed in alloys C, C-276, C-22, X, B, and 625 was isomorphous with that of Mo_6Co_7 (JCPD card no. 29–489, hexagonal: $a = 0.476$ nm and $c = 2.562$ nm). As an example, Table III summarizes the observed d-spacings of μ-phase formed in alloy C-276 after 1 h exposure at 870 °C in comparison with those of JCPD card file no. 29–489. Corresponding selected-area diffraction patterns in different orientations are

TABLE III Observed d-spacings of μ-phase in Alloy C-276 in comparison with those of Mo_6CO_7 (JCPD card file no. 29–489, $a = 0.476$ nm and $c = 2.562$ nm)

hkl	d_{obs}(nm)	$d_{JCPD\,29-489}$(nm)
003	8.54	8.532
006	4.30	4.267
101	4.09	4.070
104	3.48	3.466
018	2.54	2.529
110	2.40	2.381
113	2.33	2.293
1010	2.19	2.176
0012	2.15	2.135
116	2.10	2.080
021	2.06	2.055
0111	2.04	2.027
024	1.29	1.281
205	1.27	1.264

illustrated in Fig. 1. All patterns were consistently indexed in terms of the above structure. Owing to the complexity of the crystal structure of the μ-phase, it was not possible to check the absence of certain reflections. However, consistent with the results of XRD, (0002), (0004), ... , etc. reflections were not detected, which could be related to the characteristic layer structure of the μ-phase parallel to the basal plane [4]. Instead, (0003), (0006), ... , etc. reflections were observed. Normal to the basal plane, $(10\bar{1}0)$, $(20\bar{2}0)$, $(30\bar{3}0)$, ... , etc. reflections were detected in electron diffraction patterns, however, only the $(30\bar{3}0)$ reflection was reported in X-ray diffraction patterns. Possibly, those reflections could be due to atomic order, which were not detected in X-ray diffraction patterns. Although a μ-phase of the type Mo_6Ni_7 is not thermodynamically stable, it is shown below that it could be stabilized by the presence of iron.

Fig. 2 summarizes the results of analysing a μ-phase particle formed in alloy C-276 after 1 h exposure at 870 °C. Characteristically, the μ-phase had a banded structure such as that shown in the bright-field STEM image of Fig. 2a. As suggested by the energy dispersive spectrum of Fig. 2b, the composition of the μ-phase was of the type Mo_6Ni_7, however, it contained a marked concentration of iron, and smaller concentrations of cobalt and chromium. Because both iron and cobalt tend to lower the e/a ratio, they could stabilize such a μ-phase. However, because alloy C-276 contains a greater concentration of iron (see Table I), it would be expected to be the major stabilizer of a nickel-based μ-phase. From the spectral data of Fig. 2b, the μ-phase appeared to be of the type $(Mo, W)_6(Ni, Co)_7$ containing a small concentration of chromium.

Generally, the μ-phase particles were attached to pre-existing molybdenum-rich carbide particles of the type M_6C or $M_{12}C$ (M is a metal corresponding to Ni_3Mo_3 or Ni_6Mo_6) as shown by Fig. 2a and c, which could be related to the similarity in their crystal structures [2]. Each carbide was distinguished by its lattice constant (M_6C, face-centred cubic: $a = 1.11$ nm, and $M_{12}C$, face-centred cubic: $a = 1.09$ nm). It is shown later, that the bands of Fig. 2a correspond to twin-

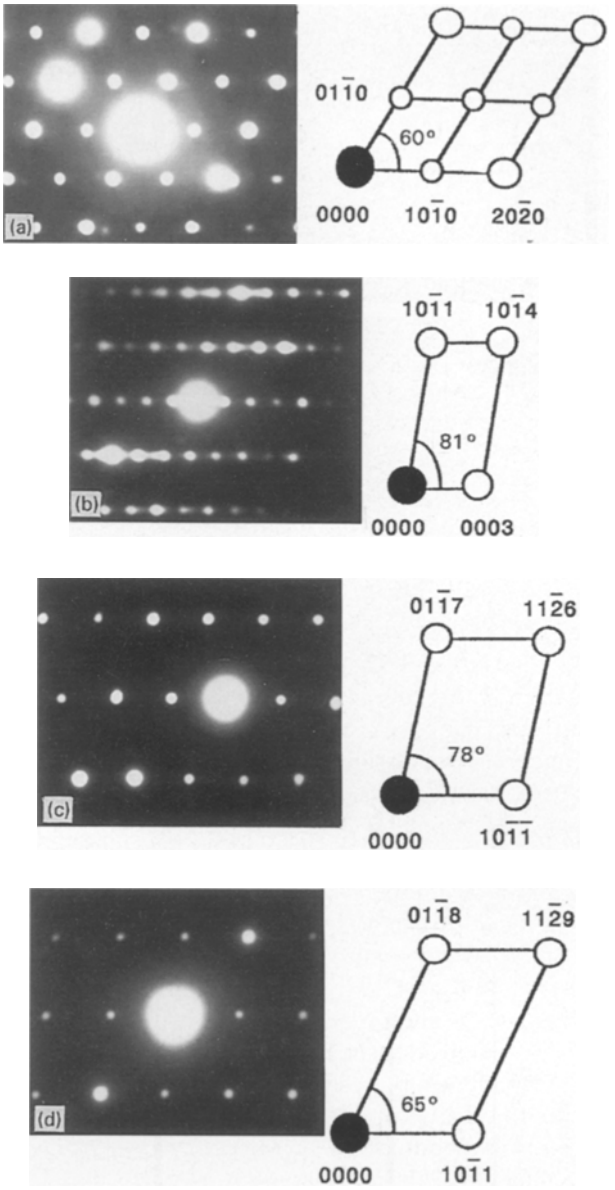

Figure 1 Selected-area diffraction patterns derived from a μ-phase particle in alloy C-276 (1h/870 °C) at different orientations. (a) [0001] orientation, (b) $[01\bar{1}0]$ orientation, (c) $[1\bar{8}91]$ orientation, (d) $[1\bar{7}61]$ orientation.

related crystals. By comparing the spectra of Figs 2d and e, it could be concluded that precipitation of μ-phase had resulted in localized depletion of molybdenum. This was further confirmed by high-resolution lattice imaging, as summarized in Fig. 3, where the d-spacing of the $\{111\}_{matrix}$ planes can be seen to decrease as the μ-phase particle was approached.

Figs 4 and 5 illustrate the identification of twins and faults parallel and normal to the basal plane within the μ-phase. Sequential faults parallel and normal to the basal plane are characteristic features of μ-phase and other related phases [5].

Alloys C, C-22, B, and 625 exhibited a behaviour similar to that of alloy C-276 as described above. For example, Fig. 6 illustrates that the μ-phase formed in alloy B after 16000 h exposure at 540 °C was of the type $Mo_6(Ni, Fe)_7$. It is recalled from Table II that the closely related alloy B2 was not susceptible to precipitation of μ-phase, which could be related to its small concentration of iron ($\leq 2\%$) in comparison with

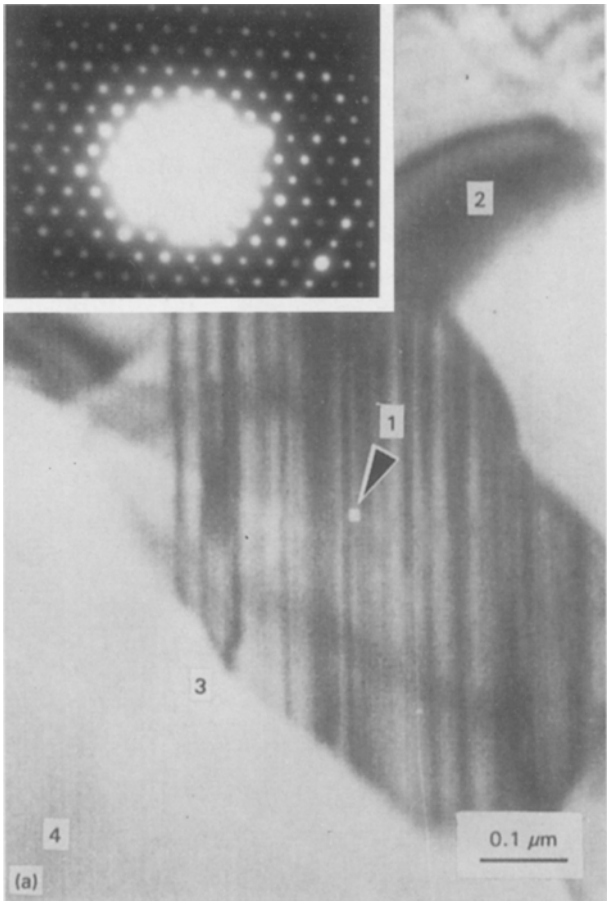

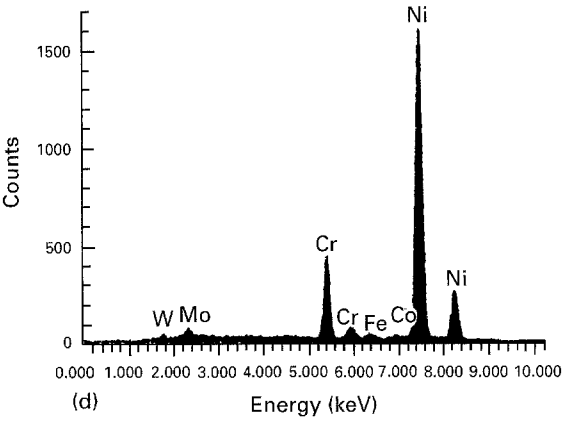

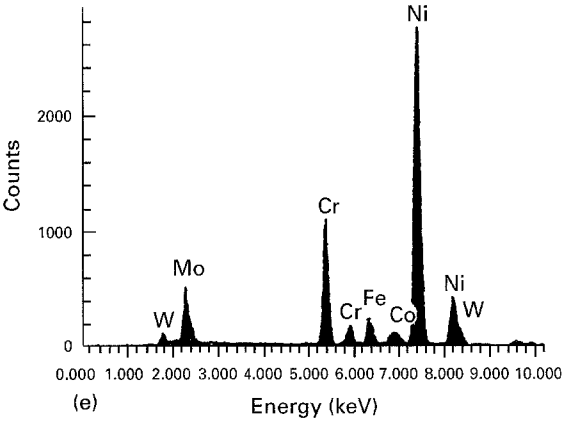

Figure 2 Analysis of μ-phase composition in alloy C-276, (1 h/870 °C). (a) Bright-field STEM image and [0 0 0 1] microdiffraction pattern. (b–e) Energy dispersive X-ray spectra derived from the regions marked (b) 1, (c) 2, (d) 3, and (e) 4 in (a).

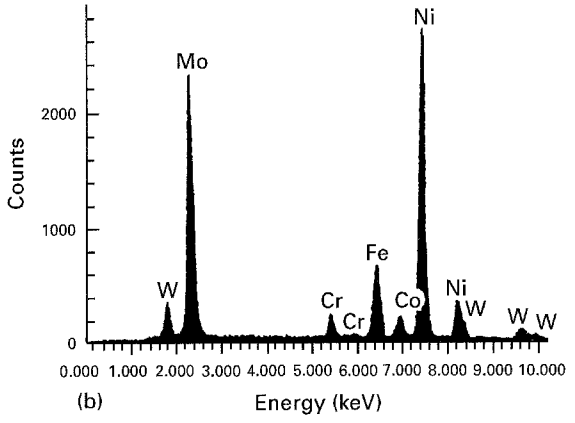

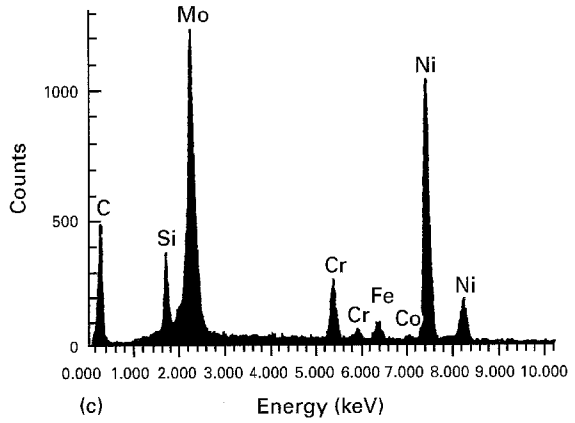

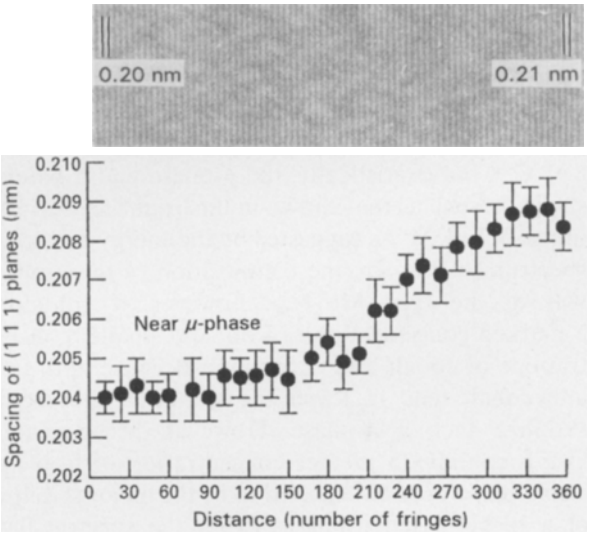

Figure 3 High-resolution lattice image of {1 1 1} matrix planes in the vicinity of a μ-phase particle in alloy C-276 (1 h/870 °C) and corresponding profile of *d*-spacing.

alloy B (5% Fe). Similarly, the relatively low iron contents of alloys C-4 and S ($\leq 3\%$) in comparison with alloys C (5.5% Fe), C-276 (5.5% Fe), and C-22 (3% Fe) could explain their resistance to precipitation of μ-phase. Also, the low iron content of alloy 230 ($\leq 3\%$) could explain its resistance to precipitation of μ-phase although its tungsten content is relatively high, further confirming that a critical concentration of iron is needed to stabilize a μ-phase of the type Mo_6Ni_7 or W_6Ni_7. Alloy 625 exhibited a rather different behaviour. Heats of the alloy containing $\leq 3\%$ Fe

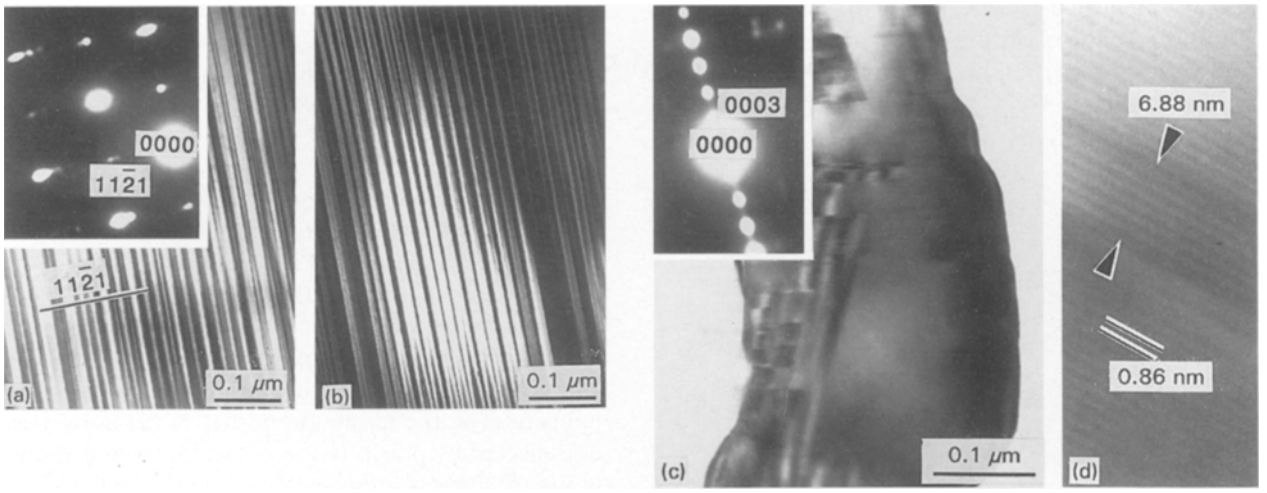

Figure 4 Planar imperfections in the μ-phase (alloy C-276, 1 h/870 °C). (a) Bright-field TEM image and corresponding $[1\,1\,\bar{2}\,2]$ diffraction pattern. (b) Dark-field image formed with the encircled reflection in (a) showing twins on $\{1\,1\,\bar{2}\,1\}$ planes. (c) Bright-field TEM image and corresponding diffraction pattern near [0 0 0 1] orientation. (d) Lattice image of (0 0 0 3) showing planar faults on the basal plane.

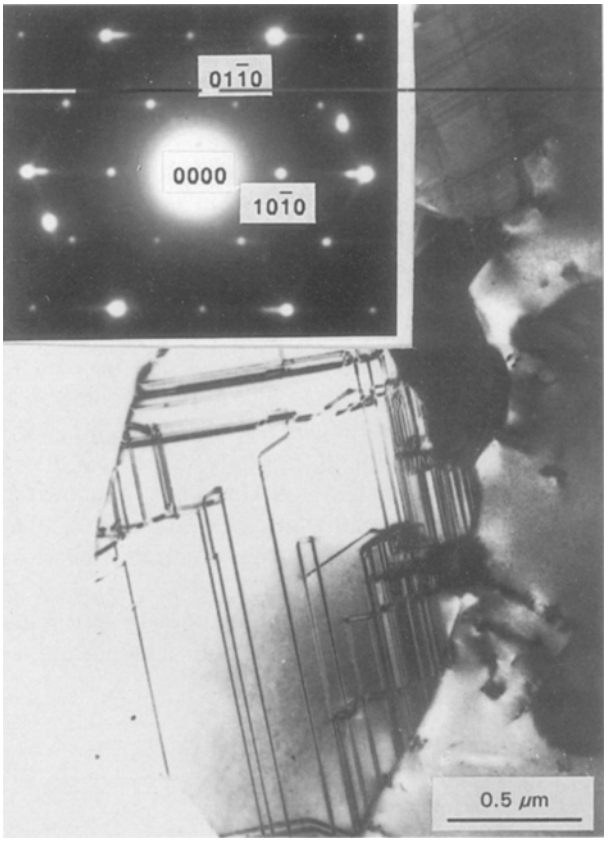

Figure 5 Planar faults normal to the basal plane of a μ-phase particle at a grain boundary; an $M_{12}C$ carbide particle can be seen attached to the μ-phase particle. Bright-field TEM image and [0 0 0 1] diffraction pattern showing streaks along $\langle 1\,0\,\bar{1}\,0 \rangle$ directions (alloy X, 100 h/870 °C).

were not susceptible to precipitation of μ-phase. However, μ-phase was detected in heats containing greater than 3% Fe. In the case of alloy X, the μ-phase was found to be of the type Mo_6Fe_7 containing nickel and cobalt, which could be correlated with the high iron content of the alloy (18.5%). Based upon the above results, the critical iron concentration required to stabilize the μ-phase appeared to be in excess of about 3%.

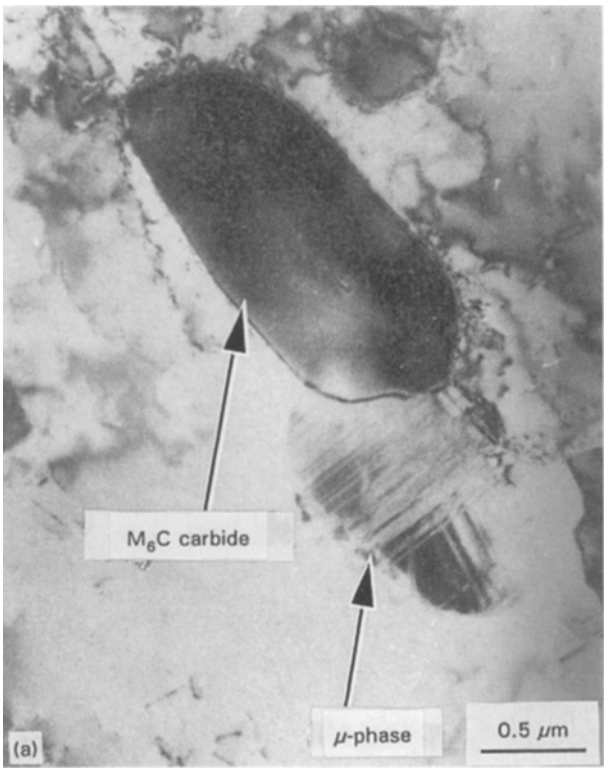

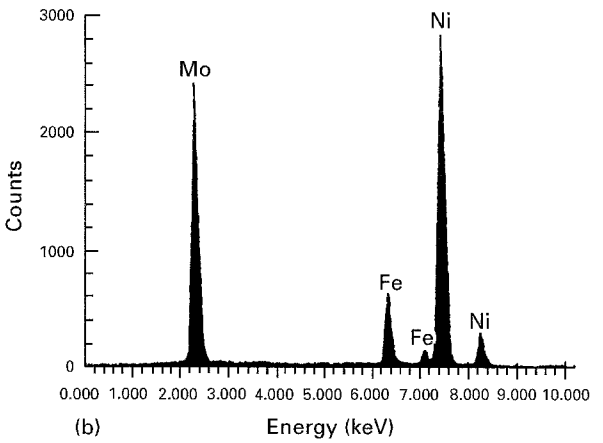

Figure 6 Iron-stabilized μ-phase in the matrix of alloy B, (16 000 h/540 °C). (a) Bright-field STEM image; an M_6C carbide particle can be seen attached to the μ-phase particle. (b) Energy dispersive spectrum derived from the μ-phase particle in (a).

3.3. Effect of μ-phase on properties

To illustrate the effect of precipitation of μ-phase on mechanical properties, Fig. 7 summarizes the effect of exposure time at 870 °C on the tensile properties and impact toughness of alloy X. As can be seen from Fig. 7a the room-temperature tensile ductility was reduced by precipitation of μ-phase; however, the alloy still maintained about 23% elongation after 16 000 h exposure corresponding to about 50% tensile ductility in the annealed condition. An overageing effect was observed after about 1000 h exposure, which could be correlated with growth of the μ-phase. In contrast with tensile properties, the room-temperature impact toughness was significantly affected by precipitation of μ-phase as illustrated in Fig. 7b. As can be seen, the Charpy impact energy was decreased from about 130 J in the annealed condition to about 20 J after 16 000 h exposure at 870 °C. At elevated temperatures, the tensile properties of the alloy were not affected by precipitation of the μ-phase as shown in Fig. 7c. Possibly, this behaviour could be due to an order–disorder reaction within the μ-phase [3]. Qualitatively similar results were obtained in the case of alloys C, C-276, and C-22.

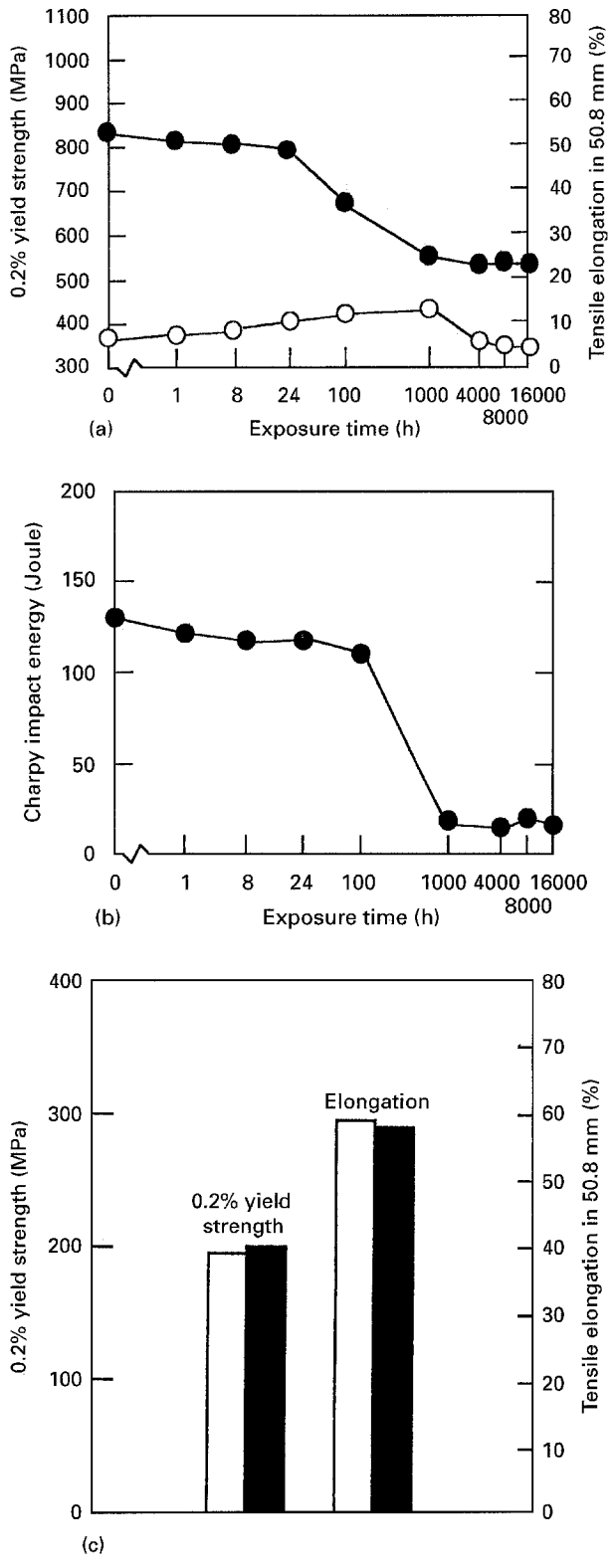

Figure 7 Effect of exposure time up to 16 000 h at 870 °C on the mechanical properties of alloy X. (a) Room-temperature tensile properties: (○) 0.2% yield strength, (●) tensile elongation. (b) Room-temperature Charpy V-notch impact toughness. (c) Tensile properties (□) before and (■) after 16 000 h exposure at 870 °C.

The difference in behaviour between Ni–Mo–Cr alloys containing relatively high iron concentration, such as alloys C, C-276, C-22, and certain heats of alloy 625 and those containing a smaller concentration of iron, e.g. alloys C-4 and S, is exemplified by the Charpy impact data of Fig. 8. Although alloy C-276 had suffered a considerable loss of room-temperature impact toughness after exposure at 870 °C, alloy C-4 (not susceptible to precipitation of μ-phase) can be seen to maintain its toughness after up to 16 000 h exposure. A similar effect was reflected by the comparative corrosion properties of the two alloys as shown in Fig. 9. After 1 h exposure at temperatures in the range of 540–870 °C, alloy C-4 can be seen to maintain its corrosion resistance in both boiling 10% HCl (Fig. 9a) and boiling 50% H_2SO_4 + 42 g l^{-1} ferric sulphate (Fig. 9b). In contrast, alloy C-276 had suffered a substantial loss of corrosion resistance in both media, particularly after exposure at 870 °C, which could be related to precipitation of μ-phase as described below.

Degradation of mechanical strength by precipitation of μ-phase particularly at room temperature, as

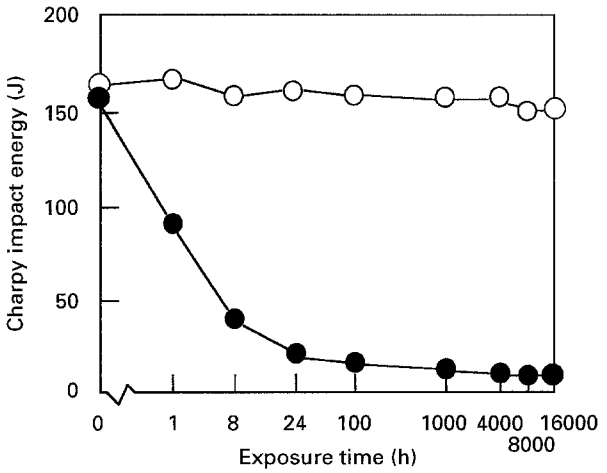

Figure 8 Effect of exposure time up to 16 000 h at 870 °C on the room-temperature Charpy impact energy of alloys (●) C-276 and (○) C-4.

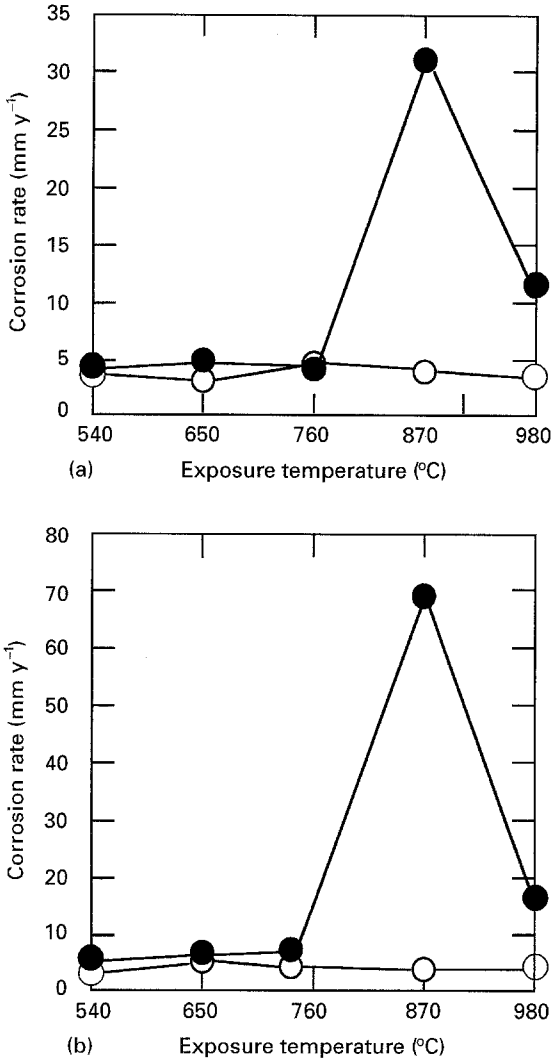

Figure 9 Effect of 1 h exposure at 650–980 °C on the corrosion properties of alloys (●) C-276 and (○) C-4. (a) Boiling 10% HCl, (b) boiling 50% H_2SO_4 + 42 g l^{-1} ferric sulphate.

demonstrated above, could be related to its high hardness and brittleness [6, 7]. This could be associated with the complex crystal structure of μ-phase and possibly atomic order. Also, the characteristic defect structure of μ-phase described earlier could act as an effective barrier to dislocation motion, and an easy path for crack propagation [7]. Because the reducing corrosion test in boiling 10% HCl detects Molybdenum-depleted zones, the observed increase in corrosion rate of alloy C-276 (Fig. 9a) could be caused by the localized depletion of molybdenum in the vicinity of μ-phase particles (Figs 2 and 3). Likewise, the oxidizing corrosion test in 50% H_2SO_4 + 42 g l^{-1} ferric sulphate detects molybdenum-rich phase such as the μ-phase explaining the observed increase in corrosion rate (Fig. 9b).

3.4. Role of alloy chemistry

It is evident from the above observations that the susceptibility to precipitation of μ-phase is a sensitive function of alloy chemistry. Although a μ-phase of the type Mo_6Ni_7 is not thermodynamically stable, the results of this study suggested that it could be stabilized by the presence of critical concentrations of iron lowering the e/a ratio.

Reference to Tables I and II indicates that alloys which were not susceptible to precipitation of μ-phase at least within the temperature range and exposure times studied (C-4, S, 230, and certain heats of alloy 625) contained small concentrations of iron typically less than 3%. This suggested that iron in excess of about 3% could stabilize μ-phase in nickel-base alloys containing molybdenum and/or tungsten by lowering the e/a ratio.

Noting that nickel deters the formation of μ-phase, Fig. 10 illustrates the susceptibility to its precipitation in the alloys studied as a function of the Ni/Fe + Co ratio versus the concentration of Mo + W. For a given (Mo + W) concentration, precipitation of μ-phase appears to be suppressed by increasing the Ni/Fe + Co ratio in the alloy. However, as the Mo + W concentration increases, a higher ratio of Ni/Fe + Co is required to prevent its precipitation. Alternately, for a given Ni/Fe + Co ratio, the susceptibility to precipitating μ-phase increases with the Mo + W concentration.

Because refractory transition elements such as molybdenum and tungsten are known to have low mobility in nickel-base alloys, it would be expected that the rate of μ-phase precipitation in a given alloy was governed by the diffusivity of these elements. Therefore, the precipitation kinetics were influenced at least partially by the concentrations of molybdenum and tungsten. This could explain, at least partially, the observed difference in kinetics between alloys C, C-276, and C-22 (about 16% Mo + W) and alloy X (about 9.5% Mo + W). However, in the case of alloy B containing a high molybdenum concentration, the sluggish precipitation kinetics could possibly be

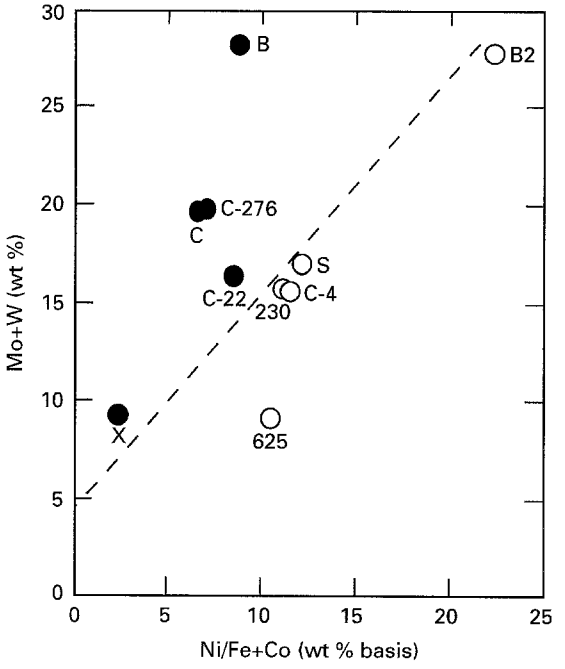

Figure 10 Susceptibility to precipitation of μ-phase in the alloys studied as a function of the Ni/Fe + Co ratio and Mo + W concentration (see Table II). (●) μ-phase, (○) no μ-phase.

related to the lower temperature range over which μ-phase was stable.

4. Conclusion

It could be concluded from the results of this study that a μ-phase of the type Mo_6Ni_7 in nickel-base alloys containing molybdenum and/or tungsten could be stabilized by the presence of critical concentrations of iron in excess of about 3%. In general, the μ-phase was distinguished by a characteristic defect structure consisting of twins and stacking faults, and it exhibited a preferential tendency for precipitation at pre-existing molybdenum-rich carbides both within the alloy matrix and at grain boundaries. Although the precipitation of μ-phase had produced a moderate loss of room-temperature tensile ductility, it caused a considerable degradation of impact toughness and corrosion resistance in both reducing and oxidizing media. However, it had no significant effect on elevated temperature tensile strength. A correlation was found to exist between the susceptibility to precipitation of μ-phase and the Ni/Fe + Co ratio as well as the Mo + W concentration. For a given Mo + W concentration, the formation of μ-phase could be suppressed by increasing the Ni/Fe + Co ratio.

Acknowledgements

It is a pleasure to acknowledge the support of the Research Institute of King Fahd University of Petroleum and Minerals and its permission to publish this work. The materials used in this study were kindly provided by the Haynes International Company.

References

1. H. M. TAWANCY, "Structure and Properties of High-Temperature Alloys: Applications of Analytical Electron Microscopy", (KFUPM Press, Dhahran, Saudi Arabia, 1993) p. 185.
2. C. T. SIMS, in "Superalloys II", edited by C. T. Sims, N. S. Stoloff and W. C. Hagel (Wiley Interscience, New York, 1987) p. 217.
3. G. WALLWORK and J. CROLL, in "Reviews of High Temperature Materials" Vol. III (2), edited by J. B. Newkirk (Freund, London, 1976) p. 69.
4. R. F. DECKER and S. FLOREEN, "Precipitation from Iron-Based Alloys" (AIME, Cleveland, OH, 1963) p. 69.
5. C. S. BARRETT and T. B. MASSALSKI, "Structure of Metals" (McGraw-Hill, New York, NY, 1966) p. 266.
6. J. H. WESTBROOK, "High Temperature Materials" (AIME, Cleveland, OH, 1965) p. 95.
7. L. R. WOODYATT, C. T. SIMS and H. J. BEATTIE, *Trans. AIME* **236** (1966) 519.

Received 20 September 1995
and accepted 15 January 1996